

# Dirhodium Catalysts That Bear Redox Noninnocent Chelating Dicarboxylate Ligands and Their Performance in Intra- and Intermolecular C–H Amination

Katherine P. Kornecki<sup>[a]</sup> and John F. Berry<sup>\*[a]</sup>

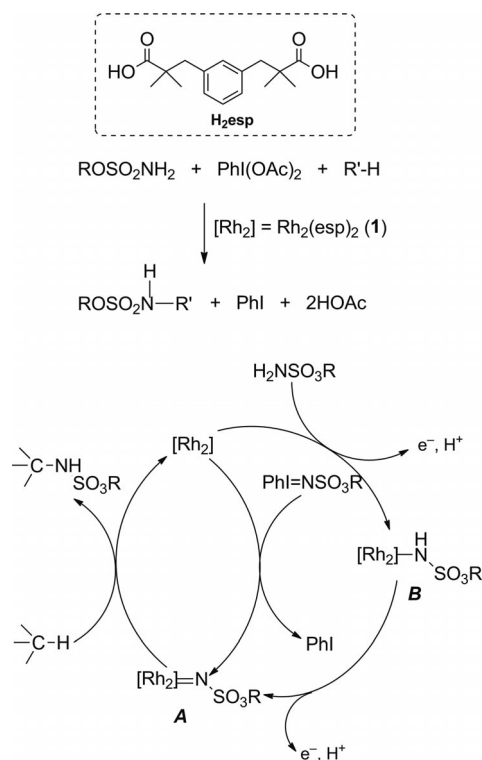
**Keywords:** Rhodium / Homogeneous catalysis / Amination / Redox chemistry / Chelates

We report two new analogues of the well-known C–H amination catalyst  $[\text{Rh}_2(\text{esp})_2]$  (**1**) ( $\text{esp} = a, a, a', a'$ -tetramethyl-1,3-benzenedipropanoate) that bear redox-active supporting ligands that are structurally similar to **esp**. The redox-active ligands are 2-[3-(1-carboxy-1-methylethoxy)phenoxy]-2-methylpropanoic acid ( $\text{H}_2\text{L1}$ ) and (3-methoxycarbonyl-2,5-di-*tert*-butylphenoxy)ethanoic acid ( $\text{H}_2\text{L2}$ ), which react with  $\text{Rh}_2(\text{OAc})_4$  to form the catalysts  $[\text{Rh}_2(\text{L1})_2]$  (**2**) and  $[\text{Rh}_2(\text{L2})_2]$  (**3**). Both **2** and **3** have been characterized by X-ray crystallography and cyclic voltammetry, *inter alia*. Compounds **2** and **3** are structurally similar to **1** but show more complex electrochemical features. Whereas **1** has a single reversible redox wave that corresponds to the  $\text{Rh}_2^{\text{II,II}}/\text{Rh}_2^{\text{II,III}}$  couple, **2**

and **3** show multiple oxidations that are characteristic of ligand-centered oxidation. Catalysts **1**, **2**, and **3** perform well in a model intramolecular C–H amination reaction, and all three catalysts perform equally well during the first four hours of a model intermolecular reaction. After this point, **2** and **3** cease to function, whereas **1** continues to be active. These results support the hypothesis that intermolecular C–H amination utilizes two distinct mechanisms: (1) a nitrene interception/insertion mechanism that is fast but ceases to be operative after four hours, and (2) a one-electron mechanism that is more robust over extended time periods, but requires the catalyst to be able to undergo  $\text{Rh}_2$ -centered oxidation.

## Introduction

Catalytic C–H amination by means of nitrene transfer mediated by dirhodium paddlewheel compounds has become an important synthetic tool.<sup>[1]</sup> This reaction is outlined in Scheme 1, and involves oxidative transformation of a nitrogen-containing substrate (typically a sulfamate or carbamate ester) into a nitrene equivalent, with subsequent insertion of this nitrene into a substrate C–H bond. The nitrene insertion can either be intramolecular, thereby yielding cyclized products, or intermolecular. Whereas intramolecular reactions are well established, it has been shown that not every  $\text{Rh}_2$  catalyst can efficiently accomplish intermolecular reactions.<sup>[2]</sup>  $[\text{Rh}_2(\text{esp})_2]$  (**1**;  $\text{esp} = a, a, a', a'$ -tetramethyl-1,3-benzenedipropanoate) has been shown to be the best catalyst for the intermolecular amination transformation,<sup>[3]</sup> a fact that has been attributed to the added stability of the catalyst due to the chelate effect of the bridging dicarboxylate ligands. Current mechanistic information on intramolecular C–H amination by **1** is consistent with the mechanism shown on the left side of Scheme 1 whereby an iminoiodinane intermediate [formed in the rate-limiting reaction of sulfamate ester with  $\text{PhI}(\text{OAc})_2$ ] transfers the ni-



Scheme 1. Proposed catalytic cycle for dirhodium-catalyzed C–H amination: the inner mechanism involves direct nitrene transfer, and the outer mechanism (with amido intermediate **B**) corresponds to the one-electron pathway that dominates the intermolecular amination mechanism.

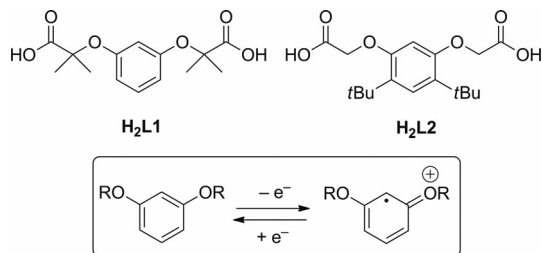
[a] Department of Chemistry,  
University of Wisconsin, Madison  
1101 University Avenue, Madison, WI 53706, USA  
Fax: +1-608-262-6143  
E-mail: berry@chem.wisc.edu

Supporting information for this article is available on the WWW under <http://dx.doi.org/10.1002/ejic.201100814> or from the author.

trene to the dirhodium catalyst, thereby yielding the dirhodium nitrene intermediate **A**.<sup>[2]</sup> Intermediate **A** is then able to insert the nitrene directly into substrate C–H bonds to reform the original catalyst. For intermolecular C–H amination reactions, the iminoiodinane transfer mechanism appears to account for only around 30% of the product formation. The majority of the product has been proposed to form by means of the outer mechanism in Scheme 1, which involves single-electron redox steps.<sup>[4]</sup> The formation of C–H amination products by using the one-electron oxidant  $Ce^{4+}$  verifies the one-electron nature of this mechanism.<sup>[4]</sup>

Redox noninnocent ligands that are strongly coupled to a transition-metal center have been employed with success in catalytic reactions that involve redox transformations.<sup>[5]</sup> To the best of our knowledge, redox noninnocence has never been studied in the context of dirhodium complexes, or the possible implications to catalysis. Ferrocene-based redox auxiliaries in dirhodium complexes have been reported, but only their electrochemistry has been studied.<sup>[6]</sup> Because of the one-electron transformations involved in the outer mechanism for intermolecular C–H amination catalyzed by  $Rh_2$  complexes, we have prepared  $Rh_2$  catalysts that bear redox noninnocent ligands and describe their performance in intra- and intermolecular amination in this article.

Since the chelate effect is touted as the reason for the increased stability and selectivity of **1** as an intermolecular amination catalyst, we decided to study catalysts that are close structural analogues of **1**. The ligands **L1** {2-[3-(1-carboxy-1-methylethoxy)phenoxy]-2-methylpropanoate} and **L2** [(3-methoxycarbonyl-2,5-di-*tert*-butylphenoxy)ethanoate] (previously reported in the context of metallomacrocyclic assembly)<sup>[7]</sup> have the same backbone chain-length as esp; however, the backbones of **L1** and **L2** contain a redox-active resorcinol-derived component (Scheme 2). Like the more well-known 1,2- or 1,4-dialkoxy-substituted benzenes,<sup>[8]</sup> 1,3-dialkoxybenzenes may be oxidized to the corresponding radical cations, as shown in Scheme 2.<sup>[9]</sup> The *meta*-disubstituted radical species are significantly less stable than their *ortho* or *para* congeners.<sup>[9,10]</sup> To the best of our knowledge, the *meta*-dialkoxybenzene motif has not yet been investigated as a redox-noninnocent ligand in coordination complexes, which further prompted this study.



Scheme 2. Chelating dicarboxylate ligands and the redox capabilities of resorcinol-based compounds.

## Results and Discussion

### Synthesis

Both  $H_2L1$  and  $H_2L2$  were previously reported by Bonar-Law and co-workers,<sup>[7]</sup> and were prepared similarly herein with slight modifications to the synthesis of  $H_2L2$  (outlined in the Exp. Section). Treating the dicarboxylate ligands with dirhodium tetraacetate at 150 °C in dichlorobenzene affords the loss of acetic acid and the formation of complexes **1–3** in good yields (60–75%). Complex formation and purity were established by  $^1H$  NMR spectroscopy, MALDI-MS, and elemental analysis. Crystals suitable for X-ray diffraction were obtained for complexes **2** and **3** as their diaquo and bis-acetone adducts, respectively (see Figures 1 and 2, *vide infra*). The axial ligands were removed under vacuum prior to the use of these compounds as catalysts.

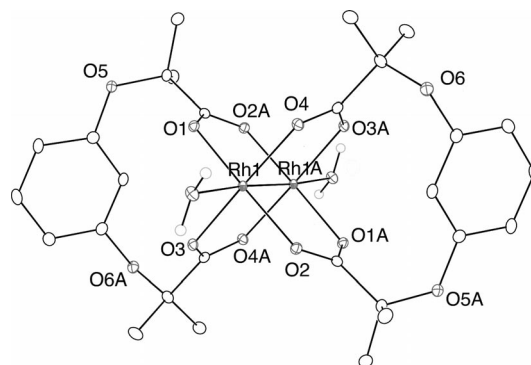


Figure 1. Thermal ellipsoid plot of catalyst **2**·2 $H_2O$ , with thermal ellipsoids drawn at the 30% probability level. Hydrogen atoms are omitted for clarity.

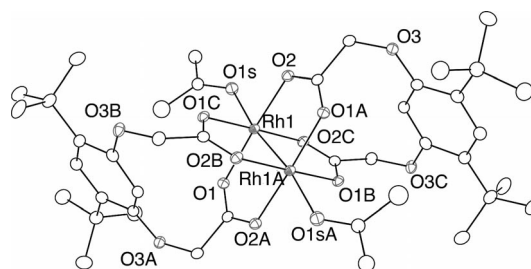


Figure 2. Thermal ellipsoid plot for **3**·2acetone, with thermal ellipsoids drawn at the 30% probability level. Hydrogen atoms are omitted for clarity.<sup>[12]</sup>

### Crystallography

Crystal data for **2** and **3** are given in Table 1. The solid-state structures of **1**, **2**, and **3** are similar and show chelation of the dicarboxylate ligands to the metal–metal bonded dirhodium core. The Rh–Rh distances in all three catalysts range from 2.3817(9) to 2.3910(6) Å, which are effectively the same (see Table 2) and fall within the normal range for bond lengths in simpler  $Rh_2^{II,II}$  carboxylate complexes.<sup>[11]</sup> The Rh–O bond lengths to the carboxylate ligands and ax-

ial ligands are all normal. An interesting difference between the three structures presents itself in a comparison of the  $O_{\text{bound carboxylate}}-C-C-O_{\text{phenolate}}$  torsion angles. There are two of these torsion angles in **1** that are crystallographically inequivalent; on one side of the bound carboxylate it is  $57.301^\circ$ , and it is  $59.238^\circ$  on the other, which are very close values and may not be considered to be significantly different in a chemical sense. This torsion angle in **3** is significantly smaller at only  $18.79^\circ$ . Interestingly, **2** differs from **1** and **3** in that its two crystallographically inequivalent smallest torsion angles on either side of the bound dicarboxylate are very different:  $99.341$  and  $37.912^\circ$ . If this difference in torsion angles is retained in solution, the nearly  $90^\circ$  torsion angle could play a role in facilitating hyperconjugation effects between the oxygen atom of the *meta*-dialkoxybenzene backbone and the carboxylate  $\pi$  orbitals, thus allowing for direct electronic communication to the rhodium center.

Table 1. Crystallographic parameters for **2** and **3**.

Compound	<b>2</b> ·2H <sub>2</sub> O	<b>3</b> ·2acetone
Space group	$P\bar{1}$	$I4/m$
Crystal system	triclinic	tetragonal
<i>a</i> [Å]	12.520(3)	19.3634(5)
<i>b</i> [Å]	12.637(3)	19.3634(5)
<i>c</i> [Å]	14.577(4)	12.1982(4)
$\alpha$ [°]	91.372(4)	90
$\beta$ [°]	100.240(4)	90
$\gamma$ [°]	101.962(4)	90
<i>V</i> [Å <sup>3</sup> ]	2215.8(10)	4573.69(2)
<i>Z</i>	2	4
<i>R</i> 1, <i>wR</i> 2 [ <i>I</i> > 2σ( <i>I</i> )]	0.0398, 0.0911	0.0302, 0.0736
<i>R</i> 1, <i>wR</i> 2 (all data)	0.0510, 0.0995	0.0446, 0.0793

Table 2. Selected bond lengths and angles in **1**, **2**, and **3**.

Compound	<b>1</b> ·2acetone <sup>[16]</sup>	<b>2</b> ·2H <sub>2</sub> O	<b>3</b> ·2acetone
Rh–Rh [Å]	2.3817(9)	2.3873(6)	2.3910(6)
Rh–O <sub>carboxylate</sub> [Å]	2.0386(18)	2.0355(2)	2.036(2)
Rh–O <sub>axial</sub> [Å]	2.3042(19)	2.298(7)	2.286(4)
O–C–O (torsion) [°]	57.301, 59.238	37.912, 99.341	18.79

## Electrochemistry

To test the redox activity of ligands **L1** and **L2**, cyclic voltammetric measurements were performed (Figures S1 and S2 in the Supporting Information). The H<sub>2</sub>esp ligand, which lacks the *meta*-dialkoxybenzene moiety, shows no redox behavior in THF up to 2.1 V versus Fc/Fc<sup>+</sup>. Under reducing conditions, an irreversible wave at  $-1.4$  V is observed. Similar reductive waves are observed in THF for H<sub>2</sub>L1 and H<sub>2</sub>L2, and it is thus reasonable to conclude that these waves correspond to electrochemical reduction and subsequent decarboxylation of the carboxylic acid functionalities. In addition to these reductive events, H<sub>2</sub>L1 and H<sub>2</sub>L2 show waves at positive potentials that correspond to oxidations that are absent in H<sub>2</sub>esp. For H<sub>2</sub>L1, multiple irreversible oxidation events are observed at potentials >1.2 V. In contrast, two discrete irreversible waves are observed for H<sub>2</sub>L2 at 0.9 and 1.1 V. The oxidations in H<sub>2</sub>L1 and H<sub>2</sub>L2 are safely assigned to the oxidation of the *meta*-

dialkoxybenzene unit. The irreversibility of the oxidations is consistent with a fast decomposition process that occurs after the radical cation is generated.

The majority of dirhodium carboxylate paddlewheel complexes exhibit one reversible redox event that corresponds to the Rh<sub>2</sub><sup>II,II</sup>/Rh<sub>2</sub><sup>II,III</sup> couple.<sup>[13]</sup> [Rh<sub>2</sub>(esp)<sub>2</sub>] (**1**) exhibits a perfectly reversible Rh-centered redox couple at  $E_{1/2} = 0.82$  V (versus Fc/Fc<sup>+</sup> in dichloromethane). Chemical oxidation and spectroelectrochemistry results indicate that this wave is centered at the Rh<sub>2</sub> unit and is assigned as the Rh<sub>2</sub><sup>II,II</sup>/Rh<sub>2</sub><sup>II,III</sup> redox couple.<sup>[4]</sup> Compounds **2** and **3** feature more complexity in their cyclic voltammograms than does **1**. In contrast to the single, reversible wave observed for **1**, compound **2** displays multiple irreversible features at >1.2 V. The irreversibility of these features and their higher redox potential than **1** suggest that these oxidation events have a different origin than the Rh<sub>2</sub><sup>II,II</sup>/Rh<sub>2</sub><sup>II,III</sup> couple of **1**. Since these redox events closely mirror the irreversible electrochemical behavior of the H<sub>2</sub>L1 ligand, it is reasonable to assign these as oxidations of the *meta*-dialkoxyphenylene moiety of the ligand backbone. Much like in the case of the free ligand itself, the radical cationic species that result from these oxidations are unstable and undergo a fast chemical reaction, likely radical/radical coupling, that renders the electrochemical signal irreversible. Like **2**, compound **3** shows multiple redox waves in its cyclic voltammogram. Unlike the irreversible behavior of **2**, the redox waves of **3** are reversible and appear at lower potentials. The CV of **3** shows a reversible two-electron wave at 0.97 V, and a further reversible one-electron wave at 1.3 V.

It is well established that phenoxy radicals and phenoxy radical complexes can be stabilized when bulky substituents protect the *ortho* and *para* positions of the aryl ring.<sup>[14]</sup> In a similar manner, addition of two *t*Bu substituents to the aryl ring of the ligands of **2** so as to form **3** leads to a greater stabilization of the corresponding radical cation [L<sub>2</sub>]<sup>•+</sup>. This stabilization is both a thermodynamic effect (reflected in the more accessible oxidation potential of **3**, 0.9 V, than **2**, >1.2 V) and a kinetic effect (the reversibility of the redox waves for **3** indicates that the chemical process responsible for rendering the **2** waves irreversible is now

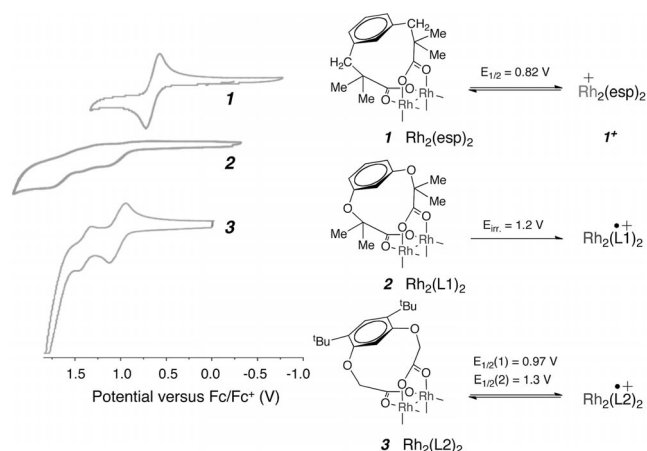
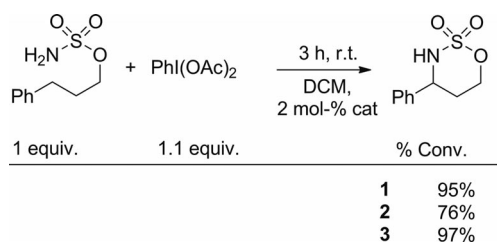


Figure 3. Redox features of chelate catalysts **1**, **2**, and **3**.

slower than the scan time of the cyclic voltammogram) (Figure 3). It is not possible to tell if one of the multiple redox waves displayed by **2** or **3** is centered at the Rh<sub>2</sub> unit. However, in comparing the electrochemical data of **1**, **2**, and **3** we may note that any Rh<sub>2</sub><sup>II,II</sup>/Rh<sub>2</sub><sup>II,III</sup> oxidations of **2** or **3** occur at substantially higher potential than in **1**, and that such an oxidation for **2** is not reversible. Given the general structural similarities between **1**, **2**, and **3**, it is not obvious why the Rh<sub>2</sub><sup>II,II</sup>/Rh<sub>2</sub><sup>II,III</sup> couple would be less accessible in the latter two compounds, but this is certainly what happens.

### Catalysis

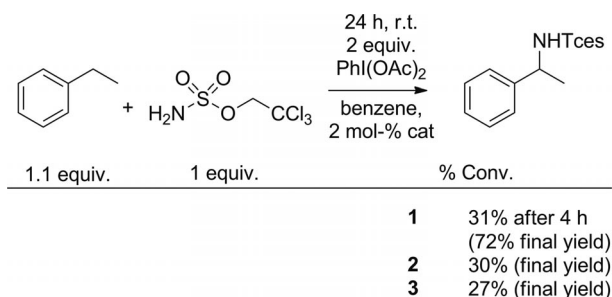
As mentioned above, catalytic amination of C–H bonds is one of the primary applications of dirhodium complexes in which their redox chemistry is proposed to play an important role. Thus the catalytic activity of **1**, **2**, and **3** in intra- and intermolecular C–H amination reactions is of interest. The reaction shown in Scheme 3 has been a useful test reaction for the performance of dirhodium catalysts in intramolecular C–H aminations that target the benzylic C–H position.<sup>[15]</sup> Simple Rh<sub>2</sub> carboxylates such as [Rh<sub>2</sub>(oct)<sub>4</sub>] (oct = octanoate) perform well as catalysts for this reaction with reported yields of approximately 84%.<sup>[15]</sup> Thus, chelating dicarboxylate ligands such as esp are not absolutely necessary for this transformation. Catalysts **1**, **2**, and **3** nevertheless perform intramolecular amination very well, particularly **1** and **3**. It is not entirely obvious why **2** gives a lower yield; however, catalyst **2** is not recoverable after the course of the reaction, thereby implying that radical reactions at the ligand may initiate catalyst degradation.



Scheme 3. Intramolecular reactivity of chelate catalysts. Percent conversion based on <sup>1</sup>H NMR spectroscopic integration versus concentration of uncyclized substrate.

To test the catalytic competence of **1–3** under intermolecular C–H amination conditions, conversion of ethyl benzene to the corresponding amination product by using H<sub>2</sub>Ntces (Tces = trichloroethylsulfamate) and PhI(OAc)<sub>2</sub> was used as a representative amination reaction (Scheme 4). Ethylbenzene is a particularly appropriate substrate since it presents benzylic C–H bonds similar to those in the intramolecular substrate described above. At four hours under these conditions, the three catalysts show comparable activity. However after this short timespan, **2** and **3** cease to function, whereas **1** continues to perform until a significant portion of the ethyl benzene is consumed. These results

complement the report from Du Bois that [Rh<sub>2</sub>(S-biTISP)<sub>2</sub>] {S-biTISP = 1,3-[N,N'-bis(2,4,6-triisopropylbenzenesulfonyl)-(2*S*,2'*S*),(5*R*,5'*R*)-proline]benzene}, despite having chelating dicarboxylate ligands, is a poor intermolecular C–H amination catalyst.<sup>[2]</sup> Due to the structural analogy between **1**, **2**, and **3**, the poor catalytic performance of the latter two can be attributed to electronic rather than steric properties. Another important piece of information about these reactions is that the brilliant red color ascribed to one-electron oxidized Rh<sub>2</sub><sup>II,III</sup> species appears when catalyst **1** is used, but is absent for reactions that involve **3**, and appears but is short-lived for reactions that involve **2**.



Scheme 4. Intermolecular reactivity of chelate catalysts. Percent conversion based on <sup>1</sup>H NMR spectroscopic integration versus an internal standard.

The catalytic results presented here can be rationalized in terms of the mechanism shown in Scheme 1 and provide further evidence to support this mechanism. Mechanistic data<sup>[15]</sup> on intramolecular C–H amination reactions are consistent with nitrene transfer from an iminoiodinane to the dirhodium catalyst, thereby forming the dirhodium nitrene complex **A**, which in turn is extremely electrophilic<sup>[16]</sup> and inserts the nitrene into the substrate C–H bond. This nitrene interception/insertion mechanism does not require any change in the oxidation state of the Rh<sub>2</sub> core, as long as **A** is considered to be an adduct of a neutral nitrene to an Rh<sub>2</sub><sup>II,II</sup> carboxylate core.<sup>[17]</sup>

At a 2 mol-% catalyst loading in the intramolecular cyclization reaction (Scheme 3), catalysts **1**, **2**, and **3** all seem to perform equally well and afford high yields of the product (>75%).

Magnesium oxide is an important additive that can affect the outcome of the reaction.<sup>[16]</sup> Table 3 gives a comparison of the yields of intramolecular C–H amination reactions catalyzed by 1 mol-% of **1**, **2**, and **3** (listed as turnover numbers) for the first 24 h of the reaction in the presence or absence of MgO. In general, catalyst performance is enhanced by this additive. We may expect that the function of MgO is to neutralize the acetic acid reaction byproduct, and that excessive amounts of acetic acid may be an important cause of catalyst arrest, particularly for **2** and **3**. Indeed, when no MgO is present, the initial green color of the dirhodium catalysts **2** and **3** quickly dissipates. Instead, the color of the reaction mixture becomes yellow, reminiscent of mononuclear Rh<sup>III</sup> species. This is not the case when **1** is used as a catalyst, thereby indicating that some facet of

its structure makes it more robust under the reaction conditions. In fact, when 1 equiv. of **1** is treated with 2 equiv. each of a sulfamate ester and  $\text{PhI}(\text{OAc})_2$  in dichloromethane, crystalline  $\mathbf{1}\cdot 2\text{HOAc}$  (see Figure S4 in the Supporting Information) can be isolated after several days, which indicates that the catalyst is unchanged by acidic conditions. Acetic acid is clearly more detrimental to catalysts **2** and **3**, possibly implicating a protonation of the resorcinol-derived O atoms and subsequent destruction of the ligand, which is not feasible when **1** is used. Notwithstanding, when MgO is present, the reaction mixture will maintain its initial green color for **2** and **3**, thus allowing all three catalysts to remain active until complete product formation is achieved, which occurs at around 20 h for catalyst **1**, and after approximately 50 h for catalysts **2** and **3**.

Table 3. Turnover numbers (TON) for the intramolecular cyclization depicted in Scheme 3 using 1 mol-% catalyst loading after 24 h.

Catalyst	TON (3 equiv. MgO)	TON (MgO-free)
<b>1</b>	99	91
<b>2</b>	86 <sup>[a]</sup>	56
<b>3</b>	69 <sup>[a]</sup>	60

[a] > 90 after about 50 h.

We<sup>[4]</sup> and Du Bois<sup>[2,3]</sup> have noted that the nature of intermolecular C–H amination catalyzed by **1** is different at the beginning of the reaction than during the later stages of the reaction. Our current hypothesis for this behavior is that intermolecular C–H amination initially occurs by means of the interception/insertion mechanism described above, but after conversion of roughly 30% of the substrate this mechanism becomes inactive and the reaction continues by following a slower one-electron mechanism. This mechanism, which dominates product formation late in the reaction, involves oxidation of **1** in the presence of sulfamate ester substrate to yield a one-electron oxidized  $\text{Rh}_2^{\text{II,III}}$ -amido-type species **B**. Species **B** has a brilliant red color and is observable as an intermediate in the reaction. It undergoes a further one-electron oxidation to yield the nitrene intermediate **A**, which inserts the nitrene into the substrate C–H bond.

The hypothesis that the nitrene interception/insertion mechanism and the one-electron mechanism operate contemporaneously is supported by results we report here. Since the nitrene interception/insertion mechanism does not involve  $\text{Rh}_2$ -centered oxidation, we expect catalysts **1**, **2**, and **3** to perform equally well in the first stage of the catalytic reaction, just as the three catalysts all perform well in intramolecular C–H amination. Indeed, this is what happens. In the first four hours of the reaction, catalysts **1**, **2**, and **3** convert around 30% of the ethylbenzene to product. The one-electron mechanism for intermolecular C–H amination requires the catalyst to be oxidized to form **B**. Both **2** and **3** are more difficult to oxidize than **1** by at least 100 mV. Moreover, one-electron oxidation of **2** or **3** does not necessarily involve oxidation of the  $\text{Rh}_2$  center from  $\text{Rh}_2^{\text{II,II}}$  to  $\text{Rh}_2^{\text{II,III}}$ , but may instead involve oxidation of the

*meta*-dialkoxybenzene ligand fragment. Neither **2** nor **3** is active in C–H amination beyond the initial four-hour period dominated by the nitrene interception/insertion mechanism. There are two possible explanations for this observation that are consistent with the working mechanistic hypothesis. First, it is possible that the one-electron oxidation of **2** or **3** occurs at such a high potential that these catalysts cannot be oxidized to **B** under the reaction conditions. The other possibility is that **2** or **3** can be oxidized under the reaction conditions, but that this oxidation is centered on the chelating dicarboxylate ligand rather than on the  $\text{Rh}_2$  unit. If the ligand oxidation is strongly coupled to the metal center, we may anticipate that **B** could still be formed under these conditions. However, there is no  $\pi$ -conjugation pathway between the *meta*-dialkoxybenzene group and the  $\text{Rh}_2$  center and a hyperconjugation pathway is doubtful, so the electronic coupling here is anticipated to be weak, thereby resulting in a one-electron oxidized species that resembles an uncoupled  $\text{Rh}_2^{\text{II,II}}$  unit appended to an organic radical cation. Such a species would not be chemically equivalent to **B**, and therefore may not take part in the one-electron C–H amination mechanism. There is some indication that both of these possibilities are, in fact, occurring. When **2** is used as a catalyst, the red color characteristic of **B** appears briefly at the beginning of the reaction, then disappears. This observation is consistent with the first possibility outlined above in which initially the concentration of oxidant is high enough that **B** can be produced, but as the concentration of the oxidant wanes, the reaction mixture no longer has sufficient oxidizing power to utilize the one-electron mechanism. In contrast, when **3** is used as a catalyst, the red color of **B** is never observed. Thus, if **3** is oxidized under these conditions, then the oxidation must be ligand-centered and there must be little electronic coupling between the *meta*-dialkoxybenzene ligand fragment and the  $\text{Rh}_2$  center. We interpret these results to mean that  $\text{Rh}_2$  centered oxidation is necessary for the success of the one-electron intermolecular mechanism, and thereby for complete conversion of substrate.

## Conclusion

For the first time, we have introduced redox noninnocent ligands as supporting ligands for metal–metal bonded compounds specifically to investigate their catalytic behavior. The *meta*-dialkoxybenzene motif in ligands **L1** and **L2** has been shown to engender the corresponding dirhodium complexes **2** and **3** with complex ligand-centered redox properties that are absent from the structurally analogous **1**. By assessing the differences in performance for catalysts **1–3**, it is evident that rhodium-centered oxidation is essential to the performance of dirhodium carboxylate catalysts in intermolecular C–H amination. Catalyst **1**, which has a reversible rhodium-centered redox couple, can access intermediate **B**, an  $\text{Rh}_2^{\text{II,III}}$ -amido species; catalysts **2** and **3** are more difficult to oxidize and are not successful in this one-electron mechanistic regime.

## Experimental Section

**General:** All reagents were obtained commercially unless otherwise noted. Reactions were performed using oven-dried glassware under an atmosphere of nitrogen, either in a glove box or using Schlenk techniques. Dichloromethane was dried with CaH<sub>2</sub> and distilled before use. [D<sub>6</sub>]Benzene was dried on an activated alumina column prior to use. All other solvents were collected anhydrous from a Vacuum Atmospheres solvent system. The structures of known compounds were confirmed by <sup>1</sup>H NMR spectroscopy and ESI-MS. <sup>1</sup>H NMR spectra were collected on a 300 MHz Bruker spectrometer at room temperature.

**Electrochemistry:** All electrochemistry experiments were conducted under a nitrogen atmosphere in solutions (10 mL, 0.1 M) of tetrabutylammonium hexafluorophosphate in freshly distilled dichloromethane with a 0.001 M analyte concentration. The reference electrode consisted of a silver wire immersed in a 10 mM silver nitrate solution contained by a Vycor tip. The auxiliary electrode was a platinum wire. For cyclic voltammetry, data was referenced to the ferrocene/ferrocenium redox couple, and the working electrode was made of glassy carbon.

**Ligands:** H<sub>2</sub>esp was prepared according to the synthesis described by Du Bois and co-workers.<sup>[18]</sup> H<sub>2</sub>L1 was prepared according to the synthesis reported by Bonar-Law and co-workers.<sup>[7]</sup> H<sub>2</sub>L2 was prepared similarly to the synthesis described by Bonar-Law and co-workers.<sup>[7]</sup> The differences are outlined below.

**Synthesis of H<sub>2</sub>L2:** Et<sub>2</sub>L2: A 100 mL Schlenk flask was charged with potassium carbonate (1.6 g, 11.6 mmol) and 4,6-di-*tert*-butylresorcinol (1.04 g, 4.7 mmol). Acetonitrile (50 mL) was added into the reaction, followed by the addition of  $\alpha$ -iodoethyl acetate (1.1 mL, 9.3 mmol). The reaction was stirred at room temperature for 40 h. Solvent was removed in vacuo, and the residue was dissolved in dichloromethane. Particulates were filtered from the dichloromethane solution, which was subsequently concentrated. Purification was achieved by means of column chromatography on silica gel with gradient elution from 5–20% ethyl acetate in hexanes to yield a clear crystalline solid (0.9 g, 24%), the ethyl ester, Et<sub>2</sub>L2. <sup>1</sup>H NMR (CDCl<sub>3</sub>):  $\delta$  = 7.229 (s, 1 H), 6.199 (s, 1 H), 4.576 (s, 4 H), 4.281 (q, 4 H), 1.387 (s, 18 H), 1.315 (t, 6 H) ppm. ESI/EMM:  $m/z$  calcd. 417.2248 [M + Na]<sup>+</sup>; found 417.2243. H<sub>2</sub>L2: NaOH (7 mL, 1 M), ethanol (5 mL), and acetone (2 mL) were added into a 25 mL round-bottomed flask charged with diester (0.4 g, 1.0 mmol). The flask was equipped with a reflux condenser and heated to 70 °C for 12 h. Any remaining ethanol was removed by rotary evaporation. A solution of 1.0 M HCl was added to the remaining reaction mixture, thereby resulting in a creamy white precipitate that was extracted into ethyl acetate (50 mL three times). The organic layer was dried with sodium sulfate, filtered, and concentrated. An off-white solid was isolated (0.31 g, 96%). <sup>1</sup>H NMR ([D<sub>6</sub>]acetone):  $\delta$  = 7.212 (s, 1 H), 6.563 (s, 1 H), 4.730 (s, 4 H), 1.392 (s, 18 H) ppm. <sup>13</sup>C NMR ([D<sub>6</sub>]acetone):  $\delta$  = 29.79, 34.32, 65.11, 99.24, 124.88, 129.78, 155.57, 169.55 ppm. ESI/EMM:  $m/z$  calcd. 337.1656 [M – H]<sup>–</sup>; found 337.1657.

**Synthesis of Dirhodium Chelate Complexes 1, 2, and 3:** Dirhodium tetraacetate·2CH<sub>3</sub>OH (100 mg, 0.197 mmol, 1 equiv.) and chelate ligand (2.5 equiv.) were added to an Erlenmeyer flask with anhydrous dichlorobenzene (30 mL). The flask was heated to 150 °C for 4 h, then allowed to cool completely. The solvent was removed by rotary evaporation, and the resulting green residue was subjected to chromatography on silica gel, gradient elution with acetone in dichloromethane, 0–25%. The complexes were afforded in 60–75% yields as microcrystalline green/green-blue solids.

**Compound 1:** Characterization data matched values previously reported by Du Bois and co-workers.<sup>[18]</sup>

**Compound 2:** <sup>1</sup>H NMR (CDCl<sub>3</sub> + 3 vol.-% [D<sub>6</sub>]acetone):  $\delta$  = 7.033 (t, 2 H), 6.464 (dd, 4 H), 6.108 (t, 2 H), 1.358 (s, 24 H) ppm. MALDI-MS:  $m/z$  calcd. 766.000; found 765.910. IR:  $\tilde{\nu}$  = 2978.91, 2962.29, 1727.29, 1596.67, 1201.36, 961.30 cm<sup>–1</sup>. Elemental analysis (2 was dried at 100 °C under vacuum to afford the complex with no axial ligation): calcd. C 43.88, H 4.21, N 0.00; found C 43.83, H 4.55, N 0.09. Crystals suitable for X-ray diffraction were obtained by dissolving the purified material in hot dichlorobenzene and allowing the solution to cool slowly (around 70 h).

**Compound 3:** <sup>1</sup>H NMR ([D<sub>6</sub>]acetone + 3 vol.-% CDCl<sub>3</sub>):  $\delta$  = 7.137 (s, 2 H), 5.202 (s, 2 H), 4.614 (s, 8 H), 1.343 (s, 36 H) ppm. MALDI-MS:  $m/z$  = calcd. 878.126; found 877.980. IR:  $\tilde{\nu}$  = 2958.67, 2914.94, 2873.92, 1592.91, 1414.18, 919.83 cm<sup>–1</sup>. Elemental analysis (3 was dried at 100 °C under vacuum to afford the complex with no axial ligation): calcd. C 49.21, H 5.51, N 0.00; found C 49.28, H 5.79, N 0.13. Crystals suitable for X-ray diffraction were obtained by dissolving the purified material in a 1:1 mixture of acetone and dichloromethane followed by slow evaporation of the solvents.

**Compound 1·2HOAc:** Crystals suitable for X-ray diffraction were isolated from the treatment of 1 (30 mg, 0.039 mmol) with trichloroethylsulfamate (18 mg, 0.078 mmol) and PhI(OAc)<sub>2</sub> (25 mg, 0.078 mmol) in dichloromethane (5 mL). The red reaction mixture was layered with hexanes. After several days, blue-green crystals were harvested.

CCDC-837373 (for 2), -837374 (for 3), and -846682 (for 1·2HOAc) contain the supplementary crystallographic data for this paper. These data can be obtained free of charge from The Cambridge Crystallographic Data Centre via [www.ccdc.cam.ac.uk/data\\_request/cif](http://www.ccdc.cam.ac.uk/data_request/cif).

**Amination Reactions:** Each of the three catalysts was tested in a prototypical intermolecular C–H amination reaction, as well as an intramolecular cyclization. For the intramolecular reaction, a prototypical reaction using the substrate depicted in Scheme 3 was performed in dichloromethane with the addition of 1.1 equiv. of hypervalent iodine oxidant, as reported in the literature.<sup>[15]</sup> The intramolecular reaction was typically complete after 4 h, as monitored by TLC. TONs were measured internally by <sup>1</sup>H NMR spectroscopy using a 1 mol-% catalyst loading over a 24 h period and by conducting the reaction described above in CD<sub>2</sub>Cl<sub>2</sub>. Product concentrations were determined against an internal cyclooctane standard.

Intermolecular reactions were performed in deuterated solvent and product formation was monitored over the course of 24 h in the presence of two equivalents of hypervalent iodine oxidant, as reported previously.<sup>[4]</sup> Final product conversion was done on the basis of <sup>1</sup>H NMR spectroscopic integration.

**Supporting Information** (see footnote on the first page of this article): Figures S1 and S2 show the cyclic voltammograms for H<sub>2</sub>L1 and H<sub>2</sub>L2; and Figures S3 and S4 show the crystal structures of 3 and 1·2HOAc.

## Acknowledgments

We thank the Chemical Sciences, Geosciences, and Biosciences Division, Office of Basic Energy Sciences, Office of Science, U.S. Department of Energy for support (grant number DE-FG02-10ER16204).

- [1] a) D. N. Zatalan, J. Du Bois, *Top. Curr. Chem.* **2010**, *292*, 347–378; b) H. M. L. Davies, J. R. Manning, *Nature* **2008**, *451*, 417–424; c) H. M. L. Davies, M. S. Long, *Angew. Chem.* **2005**, *117*, 3584–3586; *Angew. Chem. Int. Ed.* **2005**, *44*, 3518–3520.
- [2] K. W. Fiori, J. Du Bois, *J. Am. Chem. Soc.* **2007**, *129*, 562–568.
- [3] D. N. Zatalan, J. Du Bois, *J. Am. Chem. Soc.* **2009**, *131*, 7558–7559.
- [4] K. P. Kornecki, J. F. Berry, *Chem. Eur. J.* **2011**, *17*, 5827–5832.
- [5] a) P. J. Chirik, K. Wieghardt, *Science* **2010**, *327*, 794–795; b) W. Kaim, *Inorg. Chem.* **2011**, *50*, 9752–9765.
- [6] F. Estevan, P. Lahuerta, J. Latorre, E. Peris, S. Garcia-Granda, F. Gomez-Beltran, A. Aguirre, M. A. Salvado, *J. Chem. Soc., Dalton Trans.* **1993**, 1681–1688.
- [7] J. Bickley, R. Bonar-Law, T. McGrath, N. Singh, A. Steiner, *New J. Chem.* **2004**, *28*, 425–433.
- [8] J. K. Kochi, *Angew. Chem.* **1988**, *100*, 1331; *Angew. Chem. Int. Ed. Engl.* **1988**, *27*, 1227–1266, and references therein.
- [9] a) M. Jonsson, J. Lind, T. Reitberger, T. E. Eriksen, *J. Phys. Chem.* **1993**, *97*, 11278–11282; b) J. Pavlinac, M. Zupan, S. Stavber, *Org. Biomol. Chem.* **2007**, *5*, 699–707; c) J. Pavlinac, M. Zupan, S. Stavber, *J. Org. Chem.* **2006**, *71*, 1027–1032.
- [10] F. Marchetti, G. Pampaloni, C. Pinzino, *J. Organomet. Chem.* **2011**, *696*, 1294–1300.
- [11] H. T. Chifotides, K. R. Dunbar, in: *Multiple Bonds Between Metal Atoms* (Eds.: F. A. Cotton, C. A. Murillo, R. A. Walton), Springer, New York, **2005**, pp. 465–567.
- [12] The structure of **3** crystallizes with both acetone and dichloromethane as axial ligands with disorder 84% acetone/16% dichloromethane. The CH<sub>2</sub>Cl<sub>2</sub> ligand was omitted from the thermal ellipsoid plot for clarity, and is shown in Figure S3 in the Supporting Information.
- [13] K. Das, K. M. Kadish, J. L. Bear, *Inorg. Chem.* **1978**, *17*, 930–934.
- [14] P. Chaudhuri, K. Wieghardt, *Prog. Inorg. Chem.* **2001**, *50*, 151–216.
- [15] C. G. Espino, P. M. Wehn, J. Chow, J. Du Bois, *J. Am. Chem. Soc.* **2001**, *123*, 635–6936.
- [16] K. W. Fiori, C. G. Espino, B. H. Brodsky, J. Du Bois, *Tetrahedron* **2009**, *65*, 3042–3051.
- [17] J. F. Berry, *Dalton Trans.* **2011**, DOI: 10.1039/C1DT11434D.
- [18] C. G. Espino, K. W. Fiori, M. Kim, J. Du Bois, *J. Am. Chem. Soc.* **2004**, *126*, 15378–15379.

Received: August 1, 2011

Published Online: November 17, 2011